

---

## Review Article

---

# Biomimetic Dissolution: A Tool to Predict Amorphous Solid Dispersion Performance

Michael M. Puppolo,<sup>1,2,4</sup> Justin R. Hughey,<sup>3</sup> Traciann Dillon,<sup>1</sup> David Storey,<sup>1</sup> and Susan Jansen-Varnum<sup>2</sup>

Received 15 January 2017; accepted 13 April 2017; published online 30 May 2017

**Abstract.** The presented study describes the development of a membrane permeation non-sink dissolution method that can provide analysis of complete drug speciation and emulate the *in vivo* performance of poorly water-soluble Biopharmaceutical Classification System class II compounds. The designed membrane permeation methodology permits evaluation of free/dissolved/unbound drug from amorphous solid dispersion formulations with the use of a two-cell apparatus, biorelevant dissolution media, and a biomimetic polymer membrane. It offers insight into oral drug dissolution, permeation, and absorption. Amorphous solid dispersions of felodipine were prepared by hot melt extrusion and spray drying techniques and evaluated for *in vitro* performance. Prior to ranking performance of extruded and spray-dried felodipine solid dispersions, optimization of the dissolution methodology was performed for parameters such as agitation rate, membrane type, and membrane pore size. The particle size and zeta potential were analyzed during dissolution experiments to understand drug/polymer speciation and supersaturation sustainment of felodipine solid dispersions. Bland-Altman analysis was performed to measure the agreement or equivalence between dissolution profiles acquired using polymer membranes and porcine intestines and to establish the biomimetic nature of the treated polymer membranes. The utility of the membrane permeation dissolution methodology is seen during the evaluation of felodipine solid dispersions produced by spray drying and hot melt extrusion. The membrane permeation dissolution methodology can suggest formulation performance and be employed as a screening tool for selection of candidates to move forward to pharmacokinetic studies. Furthermore, the presented model is a cost-effective technique.

**KEY WORDS:** free drug; bioavailability; membrane permeation dissolution; amorphous solid dispersion; poorly water soluble.

## INTRODUCTION

The majority of drug candidates in development pipelines are compounds that demonstrate good intestinal permeability but are solubility limited (1–4). They are known by the Biopharmaceutical Classification System (BCS) as class II compounds and are amendable to bioavailability enhancement (5). Approaches such as pH adjustment, micronization, nanosuspensions, co-solvent solubilization, cyclodextrin inclusion complexation, salt formation, emulsified drug formulations, and amorphous solid dispersions (ASDs) have been used to

increase the bioavailability of BCS class II compounds by enhancing their aqueous solubility and consequently dissolution rate (6,7). ASDs have been the focal point of the aforementioned practices because of the extent at which they are able to achieve and maintain a state of supersaturation. Prolonged exposure to high concentrations of dissolved drug in the gastrointestinal tract (GIT) permits enriched *in vivo* absorption. As a result, utilization of solubility enhancement platforms is flourishing. Through all stages of development, evaluating the dissolution performance of ASDs provides an indication of *in vivo* behavior and bioavailability. Proper *in vitro* dissolution testing can convey the influence of key *in vivo* performance parameters and can be implemented for assessment and comparison of ASD formulations.

While the use of ASDs is continuously expanding, their dissolution behavior is not as well understood. The overarching objective of dissolution testing during formulation development is to achieve biological relevance and predict *in vivo* performance. Thus, an ideal dissolution method must be designed to reflect the physicochemical, physiological, and hydrodynamic

---

<sup>1</sup>Hovione LLC, 40 Lake Drive, East Windsor, New Jersey 08520, USA.

<sup>2</sup>Department of Chemistry, Temple University, 1901 North 13th Street, Philadelphia, Pennsylvania 19122, USA.

<sup>3</sup>Banner Life Sciences, 4215 Premier Drive, High Point, North Carolina 27265, USA.

<sup>4</sup>To whom correspondence should be addressed. (e-mail: michael.puppolo@temple.edu; mpuppolo@hovione.com)

conditions that transpire throughout drug dissolution and absorption during transit in the gastrointestinal tract (8,9). Predicting the *in vivo* performance of poorly water-soluble drug formulations may not be accurately accomplished employing the dissolution methodologies described in the US Pharmacopeia (USP). BCS class II drug compounds typically exhibit a solubility of <20 mg/L, which would infer an excessive amount of dissolution media or the use of a surfactant to achieve sink conditions (*i.e.*, 30 L for a 200-mg dose of drug substance with a solubility of 20 mg/L). These conditions lack physiological relevance in most cases, and therefore, depicting *in vitro-in vivo* correlation (IVIVC) or *in vitro-in vivo* relationship (IVIVR) for ASDs of BCS class II compounds is sometimes only possible under non-sink conditions.

Ideally, dissolution testing should mimic the mass transport of drug molecules across the mucosa layer and epithelial membrane, which occurs through diffusion and convection (10). The intestinal permeability of drug substances along the GIT may vary, suggesting that non-sink dissolution conditions should be explored to ensure that an excess amount of drug is available for absorption (11). A mechanistic understanding of drug speciation and performance of solubility-enhanced systems during the absorption processes is necessary to develop a predictable dissolution method. Upon solvation and as the solubility-enhanced system transports down the GIT, several higher energy drug-containing species may be present in addition to freely dissolved drug (free drug) (12). Some potential species present at non-sink conditions are drug-bile salt micelles, free polymer, polymer colloids, amorphous drug-polymer colloids, nanoaggregates, and large amorphous precipitates (13). Although these species are not absorbed *in vivo* in their native state, they are important in generating and maintaining supersaturation of the drug substance as they may function to replenish the supply of free drug as it is absorbed through the gastrointestinal membrane (5). Therefore, representative *in vitro* dissolution analysis should consider the influence of drug-containing species in addition to free drug.

Established USP dissolution apparatuses and methodologies focus on evaluation of total dissolved drug and may not be physiologically relevant for determining the amount of drug absorbed *in vivo* as they measure all drug-containing species rather than free drug. Isolating free drug either analytically or physically is a critical aspect for dissolution testing of ASDs (5). Analysis of free drug using conventional dissolution techniques can be cumbersome and time-consuming. Although various drug-polymer microstates are responsible for supersaturation of ASDs, often portions are only partially dissolved (14). In addition to these species, precipitated crystalline drug may also be present in the dissolution media. Therefore, dissolution analysis requires either filtration or centrifugation of samples, which is not guaranteed to completely remove the drug-containing species (12,14–16). These species possess particle sizes that range from as little as 10 nm to greater than 500 nm (13). Conventional filtration techniques (syringe microfiltration) with minimal membrane pore sizes of 30 nm would not sufficiently remove all species. Furthermore, Wu *et al.* assert that centrifugation techniques assume that all species in the supernatant are bioavailable (14). Centrifugation techniques rely on the sedimentation of drug-polymer species in precipitate from the supernatant. In

addition, centrifugation time and speed can significantly affect the species present in the supernatant. Ultrafiltration is a common application used during pharmacokinetic studies. Studies have also reported its use for filtration of buffered dissolution samples to analyze free drug (17). Modern methodologies such as dynamic dissolution use expensive equipment and detailed techniques, thus lacking any practical use for most researchers. Examples of these dissolution methods are TNO-TIM-1 and the dynamic gastric model (18). On-line nuclear magnetic resonance (NMR) can be used to thoroughly examine dissolution profiles indicating the presence free drug and other species (19,20). Sensible dissolution approaches isolate free drug by biphasic partitioning (lipophilic properties of the drug substance), diffusion partitioning (membrane permeation), or ultracentrifugation (molecular weight) (3,21–24). Common membrane permeation apparatuses include Ussing chambers, side-by-side  $\mu$ flux cells, and a 96-well microtitre plate sandwich. These approaches often employ cell-based (Caco-2) and cell-free (parallel artificial membrane permeability assay (PAMPA)) membrane systems to isolate and measure freely dissolved drug (25,26). Although Caco-2 and PAMPA membrane systems have demonstrated success, shortcomings such as long incubation periods during cell culturing, lipid composition dependence on drug retention, and control of the depth of the unstirred aqueous layer may limit their application (27). Alternatively, novel membrane approaches such as plasma treatment of microporous polymer membranes have been utilized for the production of biomimetic membranes (28). Plasma treatments can be exploited to manipulate specific characteristics to the surface of polymer membranes and diversify the membranes for a variety of applications.

The current work describes the development of a membrane permeation non-sink dissolution method that can provide analysis of complete drug speciation and emulate the *in vivo* performance of poorly water-soluble BCS class II compounds. The designed *in vitro* system permits evaluation of ASD formulations and offers insights into oral drug absorption. Pharmacokinetic processes such as dissolution, permeation, and absorption are replicated in the described *in vitro* system by the use of a two-cell apparatus, biorelevant dissolution media, and a biomimetic polymer membrane. The model drug selected for this work was felodipine, which is a neutral drug substance with an aqueous solubility of approximately 1 mg/mL (29). ASDs of felodipine were prepared by hot melt extrusion and spray drying techniques and evaluated by the membrane permeation non-sink dissolution method. Additionally, various parameters for the dissolution method were assessed and optimized. The particle size and zeta potential were studied during dissolution experiments to understand mechanisms of dissolution, supersaturation, and nucleation. The rank order of *in vivo* performance was predicted for ASDs.

## METHODS

### Materials

Felodipine was purchased from Vega Pharma Limited (Zhejiang, China). Hydroxypropyl methylcellulose acetate succinate grades MG and MMG (HPMCAS-MG and

HPMCAS-MMG) were kindly donated by Shin-Etsu Chemical Co., Ltd. (Tokyo, Japan). Polyethersulfone (PES) and nylon microporous polymer membranes were purchased from Sterlitech Corporation (WA, USA). Solvents and chemicals used for spray drying, *in vitro* dissolution testing, and high-pressure liquid chromatography (HPLC) analysis such as: acetone, acetonitrile, methanol, decanol, ammonium acetate, ammonium hydroxide, sodium phosphate monobasic, sodium chloride, and hydrochloric acid were purchased from VWR (NJ, USA). Fasted-state simulated intestinal fluid (FaSSIF) powder was purchased from [Biorelevant.com](http://Biorelevant.com) (London, UK). Commercial-grade tetrafluoromethane (CF<sub>4</sub>) (99.2% purity) gas was purchased from Concorde Specialty Gases (NJ, USA).

### Amorphous Solid Dispersion Preparation

#### Hot Melt Extrusion

Hot melt extrudates of felodipine were produced at 20, 33, and 50% (*w/w*) drug loading with HPMCAS-MMG. A Thermo Pharma 11 co-rotating twin-screw extruder (Thermo Scientific, USA) with a screw diameter of 11 mm and an L/D ratio of 40:1 was used for processing mixtures of felodipine and HPMCAS-MMG. Prior to extrusion, felodipine and HPMCAS-MMG were mixed thoroughly in a polyethylene bag. The blended mixture was fed volumetrically at a rate of 500 g/h into a hopper and extruded at a temperature of 160°C with a screw rotation speed of 100 rpm. The molten extrudate was quenched in an air-cooled zone and milled using a Fitzpatrick L1A Laboratory Fitzmill (The Fitzpatrick Company, IL, USA) equipped with a 0.010-in. screen, operating in a hammer forward configuration at 9000 rpm.

#### Spray Drying

Spray-dried dispersions (SDDs) of felodipine were produced at 20, 33, and 50% (*w/w*) drug loading with HPMCAS-MG. Prior to spray drying, acetone feed solutions of felodipine and HPMCAS-MG mixtures were prepared with 10% (*w/w*) concentration of solids. SDDs were produced in a laboratory-scale spray dryer—BUCHI Mini Spray Drier B-290 (BUCHI Corporation, DE, USA). The spray drier was operated with nitrogen in a single-pass mode (open loop). The aspirator was set to 100% of its capacity (maximum 40 kg/h). A flow rate of 1.0 kg/h was set to achieve atomization with nitrogen. The inlet temperature was adjusted to achieve an outlet temperature of 40°C. Solids were subjected to secondary drying in a vacuum oven with a temperature of 40°C for 24 h.

#### Modulated Differential Calorimetry

Thermal characterizations were performed on a Thermal Analysis Q2000 differential scanning calorimeter (TA Instruments, DE, USA) operating in modulated mode equipped with an autosampler and pinhole pans. Samples were prepared in pinhole pans and heated at a rate of 3°C/min from 25 to 250°C using a modulation amplitude of 1.0°C over a period of 60 s. Universal Analysis 2000 software (TA Instruments, DE, USA) was used to analyze results.

### X-Ray Powder Diffraction

Diffraction patterns were examined to detect the presence of crystalline felodipine using a Rigaku Miniflex II Desktop X-ray Diffractometer (Rigaku, TX, USA). An X-ray source (KCu $\alpha$ ,  $\lambda = 1.54 \text{ \AA}$ ) was operated at 40 kV and 50 mA. The samples were scanned from 3° to 40° on the  $2\theta$  scale using a step size of 0.01°  $2\theta$  and a rate of 1°  $2\theta$ /min. Calibration of the instrument was performed using powdered  $\alpha$ -alumina.

### Membrane Treatment

Biomimetic polymer membranes used in membrane permeation dissolution studies were produced by a novel hydrophobic plasma treatment. A PDC-32G inductively coupled plasma cleaner equipped with a PDC-32Q quartz chamber and a PDC-32T sample tray was kindly loaned from Harrick Plasma (NY, USA) for hydrophobic plasma treatments of polymer membranes. This apparatus uses a 13.56-MHz radio frequency signal to generate the plasma. Membranes were positioned on the quartz sample tray and secured by a polytetrafluoroethylene membrane holder. The system was purged with nitrogen gas and evacuated by a vacuum to a base pressure of ~500 mTorr for 5 min to remove any volatilized degradation products. Hydrophobic treatment of PES and nylon membranes was performed with CF<sub>4</sub> as a process gas. CF<sub>4</sub> was introduced to the chamber at a rate of 10 psi through a three-way needle valve. Following equilibration of the plasma chamber, the glow discharge was initiated at 18 W for 3 min. To ensure plasma uniformity, the chamber pressure was maintained at ~500 mTorr. Upon completion of the plasma treatment, the RF generator was switched off and the chamber was evacuated for 5 min before venting to atmospheric pressure. The biomimetic nature of the treated polymer membranes was established by statistical comparisons of dissolution profiles with that of porcine intestines.

### In Vitro Membrane Permeation Dissolution

A non-sink membrane permeation dissolution test was used to emulate the *in vivo* performance of solid dispersions and crystalline felodipine. A side-by-side cell (PermeGear Inc., PA, USA) was outfitted with PES and nylon membranes with a hydrophobic treatment on one surface. The hydrophobic surface of the membrane was positioned to face the acceptor cell. Donor cell and acceptor cells were composed of FaSSIF solution at pH 6.5 and decanol, respectively. The temperature of both cell compartments was maintained at 37°C. Both cells were agitated at a rate of 300 rpm using a 60-position stir plate (Variomag-USA, FL, USA). Appropriate amounts of felodipine/HPMCAS ASDs and crystalline felodipine were added to the donor cell such that non-sink conditions were fulfilled. All dissolution testing was performed in triplicate ( $n = 3$ ). Dissolution testing was performed over a time period of 300 min, and samples were obtained at intervals such as 0, 30, 60, 120, 180, 240, and 300 min. Samples acquired from the donor cell were centrifuged for 60 s at 13,500 rpm. Following centrifugation, the supernatant was diluted 1:1 (*v/v*) with acetonitrile to cease precipitation and analyzed by HPLC to determine the

concentration of felodipine in solution. Samples acquired from the acceptor cell were analyzed directly by HPLC to establish the concentration of felodipine. The flux of felodipine was determined from a plot of free drug concentration vs. time using the slope from the linear regression.

### High-Pressure Liquid Chromatography

The concentration of felodipine during dissolution testing of ASDs was measured using an Alliance HPLC (Waters Corporation, MA, USA) equipped with a photodiode array detector (PDA). Analysis was performed using a Sunfire C18 column (4.6 × 150 mm, 3.5 μm) (Waters Corporation, MA, USA). A 20 mM ammonium acetate (NH<sub>4</sub>OAc) buffer was prepared by weighing 1.54 g NH<sub>4</sub>OAc into 1000 mL of deionized water. Felodipine was analyzed using an isocratic mobile phase composed of 25/75 (v/v) 20 mM NH<sub>4</sub>OAc/methanol, a flow rate of 1.0 mL/min, a column temperature of 60°C, and a detection wavelength of 360 nm. The method has a detection limit of 0.025 μg/mL and demonstrated linearity using a standard curve in the range of (0.05–100 μg/mL) with a correlation coefficient (*r*<sup>2</sup>) of 1.000. The concentration of felodipine from *in vitro* dissolution samples was quantitated based upon a single point.

### Dynamic Light Scattering

To investigate the types of species present during dissolution testing, the particle size and zeta potential were evaluated using a Zetasizer Nano ZS90 (Malvern Instruments Ltd., Worcestershire, UK) equipped with a He-Ne 633-nm laser. An aliquot of aqueous dissolution media was collected at time points 0, 30, 60, 120, 180, 240, and 300 min and filtered through a grade no. 4 Whatman filter paper (GE Healthcare Bio-Sciences, Pittsburg, PA, USA) to remove large aggregates. Samples were analyzed at 37°C for 60 s using a glass cuvette, equipped with a dip cell (Malvern Instruments Ltd., Worcestershire, UK) during zeta potential analysis. Scattering information was detected at 173° using non-invasive back-scattering (NIBS) optics to reduce the effect of multiple scattering and dust contamination.

## RESULTS AND DISCUSSION

### Amorphous Solid Dispersion Preparation

Spray drying and hot melt extrusion (HME) technologies were chosen for production of ASDs as they represent a common focus of pharmaceutical development in an industry setting. Felodipine (trade names Plendil® and Renedil®) is a calcium antagonist with limited aqueous solubility used in the treatment of hypertension (30). It was selected as a model drug for formulation and dissolution method development studies due to its limited aqueous solubility (~1 mg/L) and hydrophobic nature (logP ~3) (4,29,31). HPMCAS is an enteric polymer that was chosen as a carrier for ASDs because of its amphiphilic nature, which results primarily from the ratio of acetyl and succinyl groups. Due to hydrophobic substituents, in its ionized form (pH >5.5), HPMCAS becomes soluble and may form colloids and aggregates that interact with a drug to maintain a

supersaturated state in aqueous media (32). Physicochemical characterization of drug-polymer mixtures is essential to ensure complete miscibility and therein, formulation stability.

Modulated DSC and X-ray powder diffraction (XRPD) results suggest the formation of felodipine and HPMCAS solid dispersions at a molecular level. Thermal analysis of extruded, spray-dried, crystalline, and amorphous material was examined to determine the glass transitions (*T<sub>g</sub>*) and melt endotherms (*T<sub>m</sub>*) (Table I). All solid dispersion systems portray amorphous features associated with a solid solution by exemplifying a single glass transition within the temperature range of the pure individual components. Diffractograms of ASDs produced from each technique are shown in Fig. 1a (SDD) and Fig. 1b (HME). Compared to a crystalline reference pattern, diffraction patterns of all ASDs are absent of any Bragg peaks, elucidating their amorphicity.

### *In Vitro* Membrane Permeation Dissolution

The primary objective of the current work was to develop a membrane permeation non-sink dissolution method that provides analysis of complete drug speciation and imitates the *in vivo* performance of poorly water-soluble BCS class II compounds. This technique offers an insight into the *in vivo* performance of ASDs, which engenders invaluable information at all stages of development.

### Membrane Permeation Dissolution Apparatus

A schematic illustration of the proposed membrane permeation dissolution apparatus can be seen in Fig. 2. The apparatus was developed to act as a membrane model of the human intestine. Dissolution testing was devised to account for the hydrodynamics of the gastrointestinal tract as well as the composition of the intestinal fluid and lumen. The designed apparatus consists of three components: a donor cell, an acceptor cell, and a membrane.

In the presented apparatus, the donor cell functions to replicate the physiological conditions in the gastrointestinal tract and is composed of biorelevant dissolution media. Studies have reported that important aspects of

**Table I.** Glass Transition Temperatures for Amorphous Solid Dispersions

Process	Formulation	<i>T<sub>g</sub></i> (midpoint) (°C)
Spray drying	1:1 Felodipine/HPMCAS	61.2
Spray drying	1:2 Felodipine/HPMCAS	66.5
Spray drying	1:4 Felodipine/HPMCAS	88.5
Hot melt extrusion	1:1 Felodipine/HPMCAS	54.2
Hot melt extrusion	1:2 Felodipine/HPMCAS	75.7
Hot melt extrusion	1:4 Felodipine/HPMCAS	85.2
–	Felodipine (amorphous)	46.5
–	Felodipine (crystalline)	146.5 <sup>a</sup>
–	HPMCAS	124.3

HPMCAS hydroxypropyl methylcellulose acetate succinate, *T<sub>g</sub>* glass transitions

<sup>a</sup> Reported as a melt transition (*T<sub>m</sub>*)

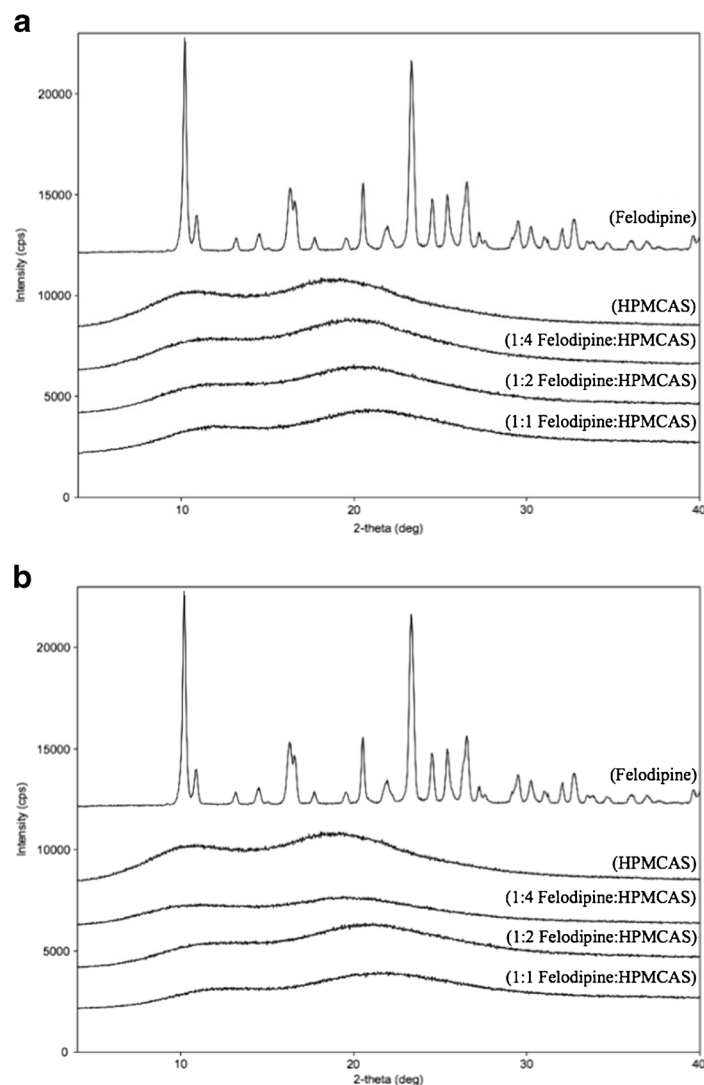


**Fig. 1.** XRPD diffractograms of **a** spray-dried and **b** extruded felodipine solid dispersions

gastrointestinal fluid include bile salt and lecithin concentrations, as well as pH considerations (8,33). FaSSIF at pH 6.5 was selected as the dissolution media for the reason that it is commonly used to evaluate oral formulations of poorly soluble compounds with regard to dissolution and solubility (34–36). Due to the solubility of felodipine in FaSSIF (~55  $\mu\text{g/mL}$ ), the donor cell is composed of a solution that exhibits non-sink conditions (34). In addition, non-sink conditions are widely accepted as more discriminating, which is more pragmatic for generating a biorelevant dissolution method (37,38).

The function of the membrane in the membrane permeation dissolution apparatus is to mimic the physiological conformation of the human intestinal epithelial membrane, which is composed of hydrophilic and hydrophobic constituents. The intestinal tract is lined with a layer of mucosa, which consists of a stratum of enterocytes (epithelium) that project villi and microvilli. The microvilli form a striated surface, which is referred to as the brush border membrane (39). The brush border membrane encompasses a stagnant layer of aqueous media that exerts a

physical barrier to lipophilic substances and is a critical aspect of transcellular absorption (40). The primary mechanism of drug absorption is passive diffusion (paracellular or transcellular). The presented work exemplifies transcellular *in vivo* absorption by passive diffusion with the use of plasma-treated microporous polymer membranes. The modified membrane generates a stagnant layer of biorelevant intestinal fluid at its hydrophilic surface as a result of a plethora of pores that promote absorption of aqueous media (Fig. 2).

The role of the acceptor cell in the proposed apparatus is to emulate an environment similar to the bloodstream. *In vivo*, the concentration of drug in the bloodstream is considered minimal as compared to the concentration in the gastrointestinal tract. Moreover, the process of diffusion can be described by Fick's law's, which conveys that the uptake of a drug substance into the bloodstream is dependent upon the concentration gradient across a membrane system and proportional to the drug lipophilicity. Therefore, to encourage permeation and absorption of free drug, the acceptor cell solution must promote sink conditions.

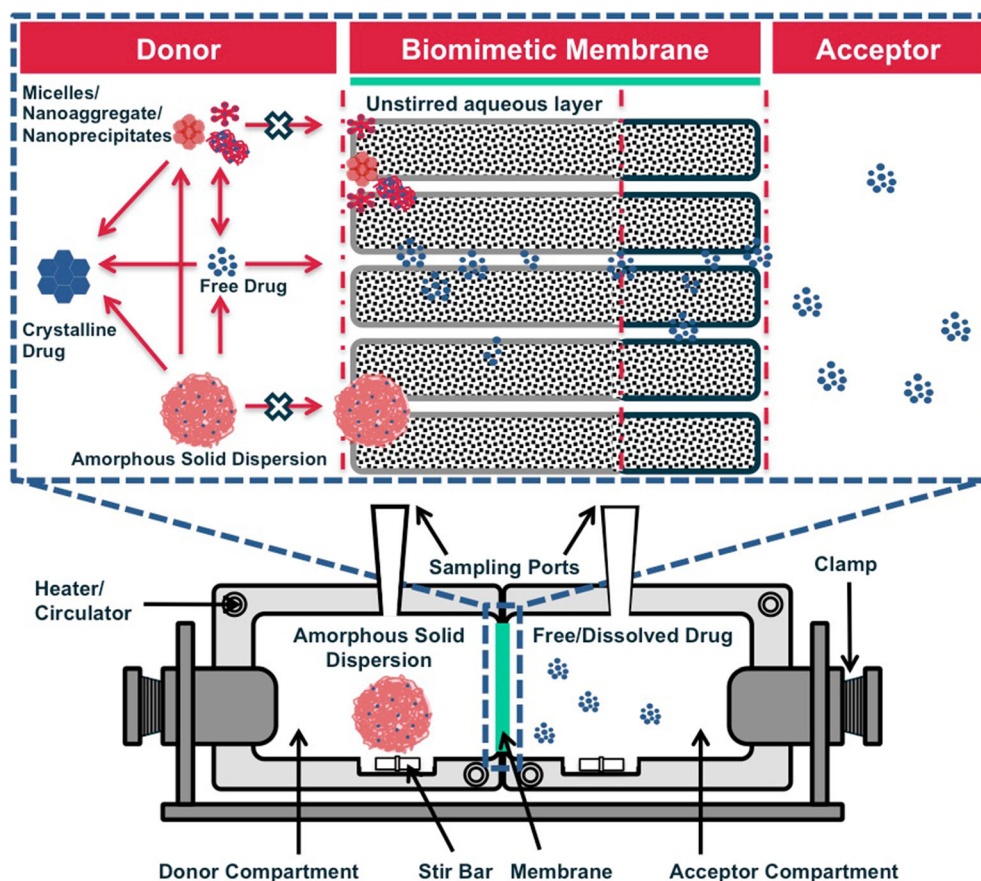


Fig. 2. Schematic illustration of the membrane permeation dissolution apparatus, unstirred aqueous layer, and hydrophobic-treated surface

### Parameter Optimization

A preliminary assessment was executed to optimize parameters critical to the dissolution apparatus and methodology. In addition to *in vivo* considerations, selected parameters were studied to determine their effective working range in the designed apparatus.

An ideal dissolution method would simulate the hydrodynamics and flow rate of the gastrointestinal tract. Insight into the unstirred aqueous layer depth and intestinal residence time can be studied through varying the agitation rate of each cell. Membrane permeation methods that have employed Caco-2 and PAMPA membranes have seen a significant dependence on the agitation rate with respect to drug permeation and absorption (41). The current work eliminates the need to investigate the correlation between agitation rate and unstirred aqueous layer thickness by fixing the depth of the hydrophilic surface in the membrane. A stir rate of 300 rpm was selected as the optimal stir rate for the apparatus (data not shown).

Porosity and pore size of a membrane can have a significant effect on the permeation and absorption of a drug substance. It is suggested that drug-containing species range in size from 20 to 500 nm (13). Nylon and PES membranes, hydrophilic by nature, with pore sizes ranging from 0.03 to 0.45  $\mu\text{m}$ , were used to investigate the most appropriate pore size for the membrane permeation dissolution apparatus after surface treatment (data not shown). At pore sizes  $\geq 0.45 \mu\text{m}$ ,

increased drug transfer was observed as a result of the inability of the larger pore sizes to adequately filter drug-containing species. Exploiting larger pore sizes can increase the number of species that enter the unstirred aqueous layer and therefore falsely enhance the likelihood of dissolution into the acceptor cell. In contrast, at pore sizes  $< 0.1 \mu\text{m}$ , a decreased drug absorption was observed and is believed to be an artifact of membrane fouling. A PES membrane with a pore size of 0.1  $\mu\text{m}$  was selected for future experiments based on its correlation with a porcine intestinal membrane.

### Application of a Biomimetic Membrane Permeation Dissolution Apparatus for Predicting Amorphous Solid Dispersion Performance

Initially, dissolution profiles of felodipine (1:4 felodipine/HPMCAS SDD) were examined to estimate the extent at which supersaturation was maintained *in vivo* (Fig. 3). The ability to monitor the concentration of felodipine in the donor and acceptor cell offers insight into mechanisms such as supersaturation, nucleation, crystallization, and diffusion. Figure 3 depicts the concentration of felodipine (1:4 felodipine/HPMCAS SDD) in the donor cell that reached a maximum of 153  $\mu\text{g}/\text{mL}$  at 180 min and precipitated slowly to a concentration of 59  $\mu\text{g}/\text{mL}$  at 1000 min. The acceptor cell in Fig. 3 exhibits a linear increase in felodipine concentration ( $R^2 = 1.000$ ) after the 180-min time point, which is indicative of supersaturation sustainment. Gautschi *et al.* suggests that

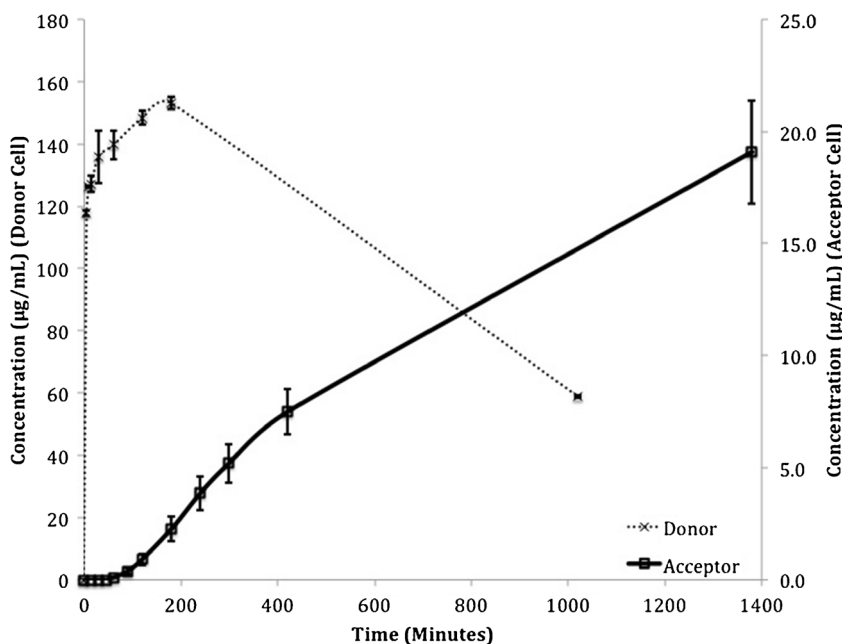


**Fig. 3.** Graphical representation of drug dissolution (donor cell) and absorption (acceptor cell) profiles against time for 1:4 felodipine/HPMCAS spray-dried dispersion. Error bars represent the standard deviation ( $n = 3$ )

formulation-derived drug species such as micelles, colloids, nanoaggregates, and nanostructures form during wetting and disintegration of the ASD and function as a potential source of free drug supply (12). The continuous elevation of felodipine concentration in the acceptor cell solution is explained by the constant replenishment of free drug in the donor cell solution from drug-containing species as felodipine permeates the membrane and is absorbed.

Up to this point, the described dissolution model has been utilized for the analysis of felodipine content in donor and acceptor cell solutions. It has been proven successful for the assessment of supersaturation and precipitation of amorphous drug from an ASD of felodipine. Sustaining drug supersaturation is a challenge frequently encountered during development work due to the unstable thermodynamic nature corresponding to the amorphous form. A critical attribute pertaining to supersaturation of an ASD is drug/polymer speciation. Understanding the influence of these species on drug supersaturation can provide fundamental information that is beneficial for optimizing formulations. Due to the design of the dissolution apparatus, particle size and zeta potential analysis of the donor cell solution can be performed to approximate the various species present and suggest their stability. Zeta potential is a measured charge revealed by any particle in a dispersed condition and is used here to offer an estimation on the degree of precipitation (42). In general, zeta potential values greater than 30 mV are representative of a stable solution due to tendency of charged particles to overcome aggregation by repelling one another (43,44). Zeta potential values less than 10 mV are symbolic of agglomeration and precipitation.

Particle size ( $z$ -average) and zeta potential values measured from the donor cell during dissolution of extruded felodipine (1:4 felodipine/HPMCAS HME) can be seen in Table II. Particle size and zeta potential values at the onset of

dissolution are challenging to interpret due to the uniformity of the donor cell media. Dissolution is described by the freeing of drug molecules from the solid phase into the liquid phase. These molecules traverse into a layer of stagnant liquid and form a saturated solution of solvent engulfing the solid molecules. As shown in Table II, the supersaturation of felodipine in 1:4 felodipine/HPMCAS extrudates occurs from 15 to 180 min. A closer evaluation of  $z$ -average particle size values reveals that values remained constant (approximately 40 nm) throughout the initial 90 min of the dissolution experiment. Friesen *et al.* report the particle size of drug-polymer nanostructures and nanoaggregates range from 20 to 100 nm and 70 to 300 nm, respectively (13). As mentioned, these species act to continuously replenish free or dissolved drug as it is absorbed into the acceptor cell. The  $z$ -average particle size values for felodipine (1:4 felodipine/HPMCAS HME) between time points 30–120-min range from 40 to 231 nm, which suggests the presence of nanostructures and nanoaggregates and justifies the presence of species known to sustain supersaturation. It should be noted that reported particle size values represent the  $z$ -average particle size of the

**Table II.** Particle Size and Zeta Potential Analysis

Time (min)	Z-average particle size (nm)	Zeta potential (mV)
15	48	-18
30	36	-20
60	41	-19
120	231	-14
180	1215	-9
240	2103	-10
300	1774	-8

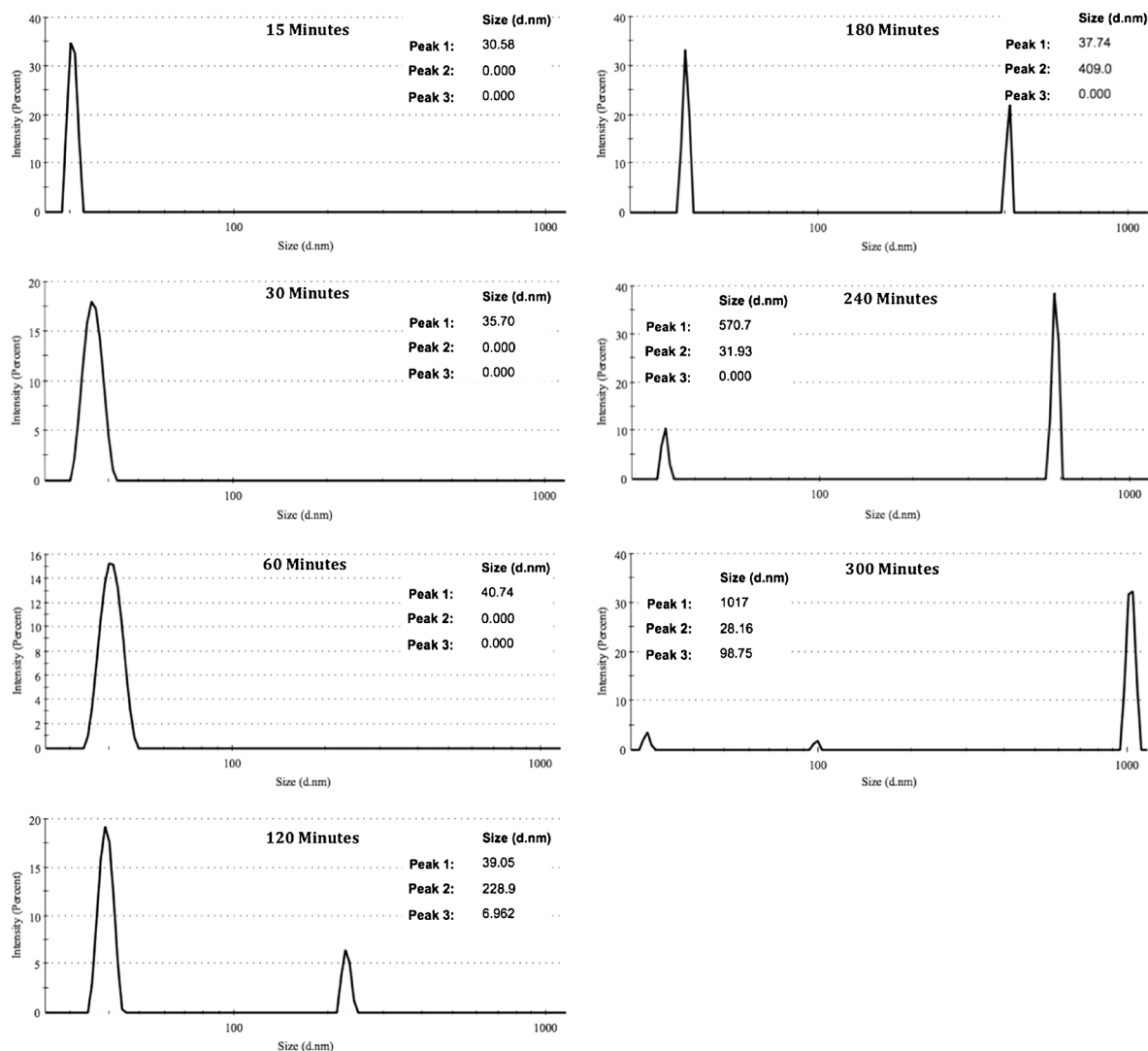


**Fig. 4.** Particle size distribution analysis of extruded felodipine solid dispersions

various species present. A closer look at the sizes of the individual species offers significant insight into supersaturation sustainment (Fig. 4). Although the *z*-average particle size values at *t* = 180 and 240 min are 1215 and 2103 nm, respectively, the majority of species present ranged from 38 to 409 nm (180 min) and 32 to 571 nm (240 min). This data

suggests that the larger particles may have interfered with the analysis during these time points, which resulted in a large *z*-average particle size value. Zeta potentials greater than 15 mV infer that the solution is thermodynamically stable (*i.e.*, precipitation from the amorphous form is not present at this point in the dissolution study). Zeta potential values were

**Table III.**  $AUDC_{(0-420 \text{ min})}$  and Flux Values for Felodipine Formulations (*n* = 3)

Process	Formulation	$AUDC_{0-420 \text{ min}}$ ( $\mu\text{g min/mL}$ )	Flux $\times 10^3$ ( $\mu\text{g}/(\text{min cm}^2)$ )	Rank
Spray drying	1:1 Felodipine/HPMCAS	2138	36.3	4
Spray drying	1:2 Felodipine/HPMCAS	3327	55.5	1
Spray drying	1:4 Felodipine/HPMCAS	2632	50.6	2
Hot melt extrusion	1:1 Felodipine/HPMCAS	2117	40.3	5
Hot melt extrusion	1:2 Felodipine/HPMCAS	2377	40.3	3
Hot melt extrusion	1:4 Felodipine/HPMCAS	2026	43.0	6
N/ap	Crystalline (0.1 mg/mL)	630	9.1	N/ap
N/ap	Crystalline (1 mg/mL)	360	3.7	N/ap
N/ap	Crystalline (10 mg/mL)	359	4.7	N/ap

HPMCAS hydroxypropyl methylcellulose acetate succinate,  $AUDC$  area under the dissolution curve, N/ap stands for not applicable

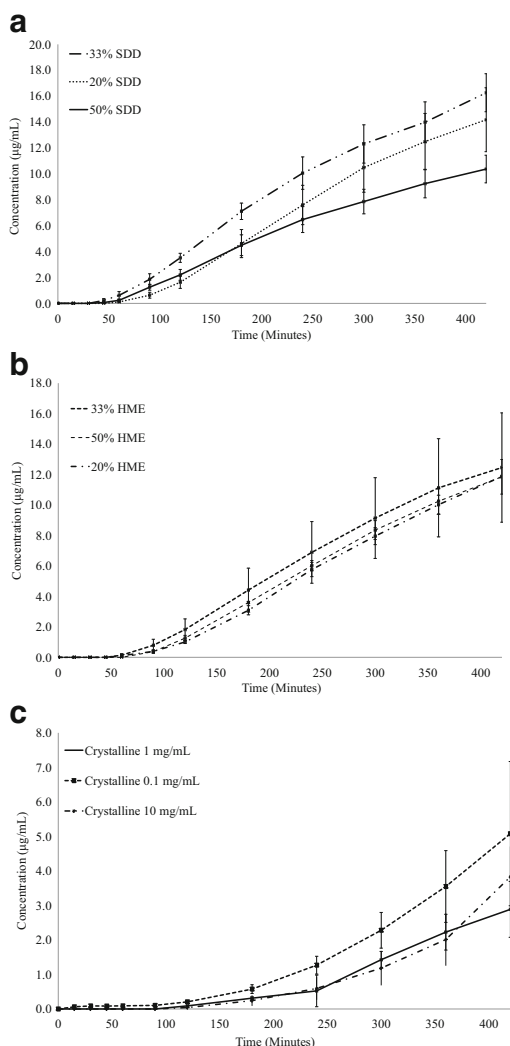


**Fig. 5.** Graphical representation of drug absorption profiles against time for **a** spray-dried, **b** extruded felodipine drug formulations, and **c** crystalline felodipine. Error bars represent the standard deviation ( $n = 3$ )

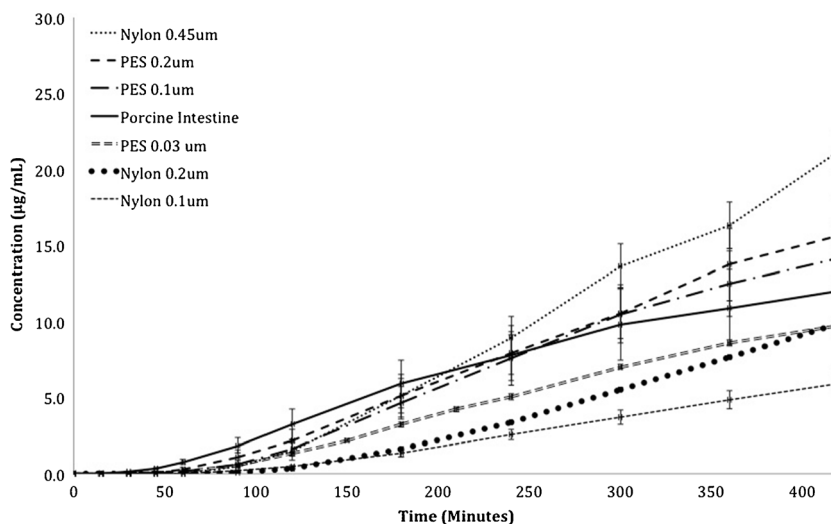


**Fig. 6.** Graphical comparison of drug absorption profiles against time using treated polymer membranes and porcine intestines for 1:4 felodipine/HPMCAS hot melt extrudates. Error bars represent the standard deviation ( $n = 3$ )

comparatively constant ( $-14$  to  $-20$  mV) over the time points ranging from 30 to 120 min, confirming that the extent of supersaturation may be a result of the species present. The formation of large precipitates is implied by the increase in the  $z$ -average particle size of the donor cell solution to 1774 nm at  $t = 300$  min. In addition,  $\sim 90\%$  of species at this time point exhibited a particle size of 1017 nm. This asserts the occurrence of nucleation of crystalline felodipine from its amorphous form. Furthermore, zeta potential values decreased to  $-8$  mV, confirming the presence of larger aggregates in solution. In conjunction with drug absorption studies, particle size and zeta potential analysis can provide invaluable information during early phase formulation development.

The oral drug absorption of felodipine can be predicted through an evaluation of the interplay between solubility and permeability in the donor and acceptor cell, respectively (2,45). Understanding the flux of felodipine through the biomimetic membrane is a critical aspect to interpreting that relationship. Equation 1 describes the flux,  $J$ , of drug molecules diffusing across the biomimetic membrane (46–48). The flux is defined as the rate of passive diffusion or the change in mass per unit time ( $\frac{dM}{dt}$ ) and is dependent upon the cross-sectional area of the membrane,  $S$ , the solute thermodynamic activity,  $a$ , the activity coefficient of the solute in the membrane,  $\gamma$ , the diffusion coefficient of the solute,  $D$ , and the membrane thickness,  $h$ .

$$J = \frac{dM}{dt} \cdot \frac{1}{S} = \frac{Da}{h\gamma} \quad (1)$$

Flux values of spray-dried and hot melt extruded ASDs can be seen in Table III. Calculations were performed at a time segment where the drug absorption into the acceptor cell demonstrated a linear value. Results indicate that ASDs with  $\sim 20$  and  $\sim 33\%$  drug loading exhibited the highest flux across the membrane and therefore absorption potential of the analyzed formulations. Overall, the SDD material provided a higher flux

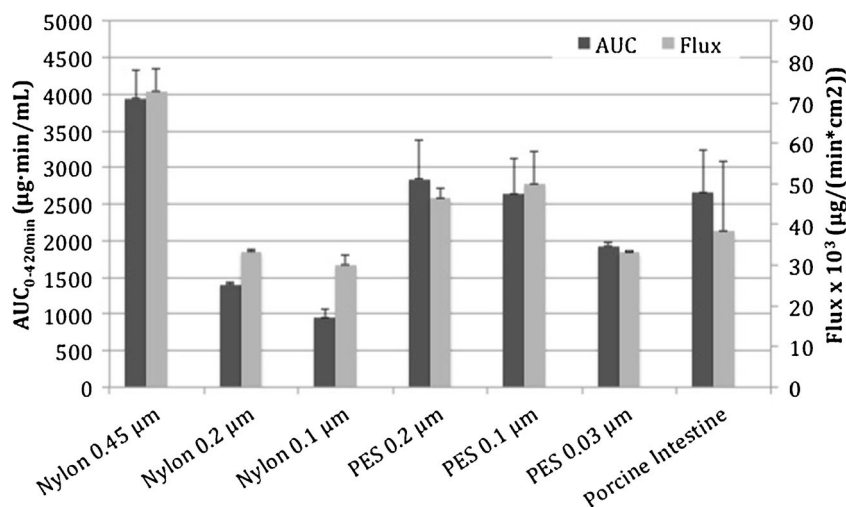


**Fig. 7.** Bar graph representation of  $AUC_{0-420 \text{ min}}$  and flux values for biomimetic membrane evaluation. Error bars represent the standard deviation ( $n = 3$ )

than HME, which is likely due to particle size (SDD  $d_{50} < 5 \mu\text{m}$ , HME  $d_{50} > 250 \mu\text{m}$ ). Analysis of flux values suggests that there was more discrimination among SDD formulations. This observation indicates that dissolution kinetics played a significant role in how fast SDD formulations dissolved and speciated. The membrane permeation dissolution apparatus and method are adept in distinguishing factors limiting drug absorption such as dissolution rate, solubility, and permeability. Possessing this capability in a research and development environment warrants more effective and biorelevant analysis of drug formulations, thus potentially reducing the amount of *in vivo* pharmacokinetic studies necessary. Additional experiments were performed to determine the effect of the amount of felodipine in the donor cell on the flux. Varying amounts of crystalline felodipine (concentrations 0.1–10 mg/mL) were added to the donor cell to attain non-sink conditions, and the flux was measured. Results in Table III denote that the amount of felodipine in the donor cell had a minimal influence on flux, and rather, the flux is a direct

function of the solubility of felodipine in the biorelevant dissolution media. Note that the slight increase in flux value for the crystalline (0.1 mg/mL) solution can be attributed to the concentration existing between non-sink and sink conditions. The flux studies proclaim the practicality of the presented membrane permeation dissolution method for evaluating the relative performance of ASDs by delineating performance as an outcome of solubility and permeability. Drug absorption profiles for the evaluated ASDs and crystalline amounts of felodipine described in Table III can be seen in Fig. 5.

### Membrane Biorelevance Evaluation

The current work describes a successful application of an *in vitro* model to predict drug absorption across the intestinal epithelial membrane. Analysis of the acceptor cell solution provides information pertaining to free drug permeation and absorption. The biorelevance of this model was established

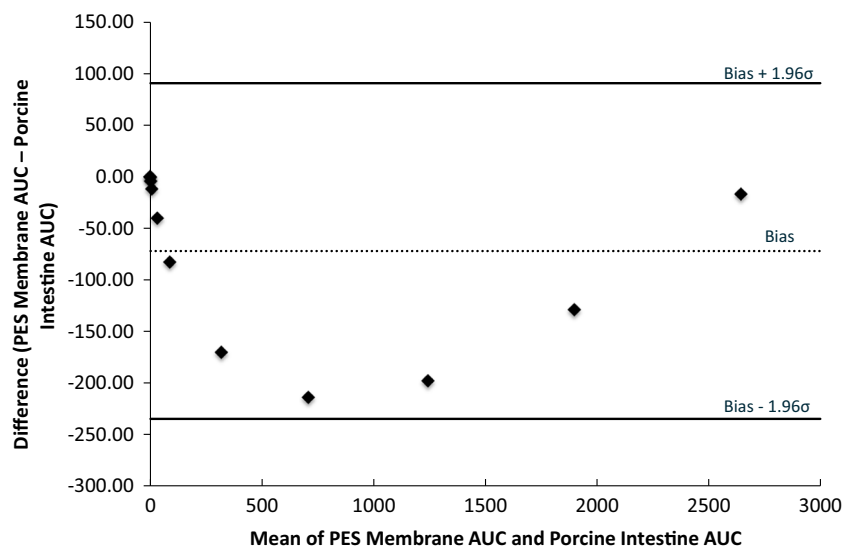


**Fig. 8.** Bland-Altman analysis of plasma-treated PES membranes and porcine intestines, where *Bias* represents the mean of the difference values and  $\sigma$  corresponds to the standard deviation of the difference values ( $n = 12$ )

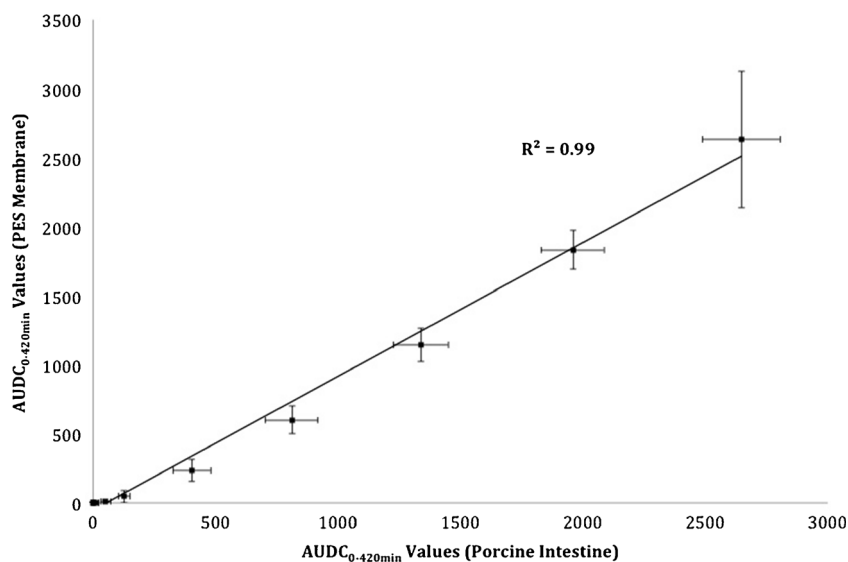


**Fig. 9.** Graphical comparison of  $AUC_{0-420 \text{ min}}$  values from drug absorption profiles of treated PES membranes and porcine intestines for 1:4 felodipine/HPMCAS hot melt extrudates. *Error bars* represent the standard deviation ( $n = 3$ )

through a comparison with a porcine intestine. Although it is challenging to obtain human intestinal tissue for equivalence studies, animal intestinal tissues are readily available and generally accepted to possess similar physiological characteristics (49).

A mechanistic study involving porcine intestinal tissue was performed to illustrate the biomimetic nature of the plasma-treated microporous polymer membranes. Drug absorption and flux values were compared (Figs. 6 and 7). The percent difference between the area under the dissolution curve ( $AUC_{0-420 \text{ min}}$ ) values for the porcine intestinal membrane compared with the  $0.1 \mu\text{m}$  PES membrane with hydrophobic treatment is less than 0.6%, indicating significant similarity between the two membranes. The Bland-Altman analysis is used to portray the agreement between two

quantitative methods of measurement (50). Furthermore, the Bland-Altman analysis is often used in support of correlation studies to assess the comparability between methods rather than a relationship between one variable. A statistical evaluation was performed to quantify the bias and range of agreement between AUC values of plasma-treated PES membranes and porcine intestines (Fig. 8). The Bland-Altman analysis of plasma-treated PES membranes and porcine intestines demonstrated that all data points fall within the 95% confidence interval, thereby illustrating an agreement between plasma-treated PES membranes and porcine intestines. Additional correlations were established to demonstrate the similarity of plasma-treated PES membranes and porcine intestines. Figure 9 illustrates a correlation of

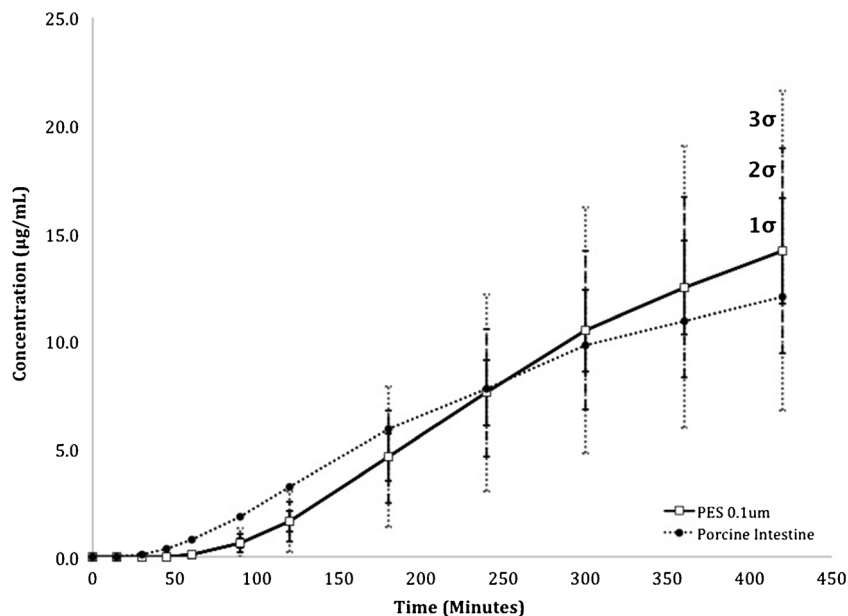


**Fig. 10.** Graphical comparison of drug absorption profiles of treated PES membranes and porcine intestines for 1:4 felodipine/HPMCAS hot melt extrudates. *Error bars* represent one, two, and three times the standard deviation ( $n = 3$ )

AUDC<sub>0-420 min</sub> values from each dissolution profile. A correlation value close to  $R^2 = 1.00$  indicates that the two dissolution profiles are similar. Figure 9 depicts a correlation value of 0.99, indicating that plasma-treated PES membranes with a pore size of 0.1  $\mu\text{m}$  are analogous to porcine intestines. Figure 10 demonstrates the standard deviation of three preparations of plasma-treated PES membranes. Assuming a normal distribution, 64% of the data should fall within one standard deviation, 95% within two standard deviations, and 99.7% within three standard deviations. Upon evaluation, it is determined that after 120 min, all time points for the porcine intestine are within one standard deviation of the plasma-treated 0.1  $\mu\text{m}$  PES membrane. In addition, the plasma-treated 0.1  $\mu\text{m}$  PES membrane exhibited equivalent AUDC<sub>0-420 min</sub> values to porcine intestines, which implies that treated membranes would predict similar bioavailability as porcine intestines. The flux values of PES membranes are typically elevated compared to equivalent pore size nylon membranes. This concludes that the hydrophobic plasma treatment was more effective on PES membranes, resulting in a reduced unstirred aqueous layer.

## CONCLUSION

The current work describes the development of a membrane permeation non-sink dissolution method that emulates the *in vivo* performance ASDs. The method has the potential to be universal with an adjustment to an appropriate pH depending on the pKa of the drug being analyzed. The membrane permeation model enables quantitative assessment of drug dissolution and absorption and offers a means to predict the relative *in vivo* performance of ASDs for BCS class II drug substances. In this work, *in vivo* pharmacokinetic processes are replicated by the use of a two-cell apparatus, biorelevant dissolution media, and a biomimetic polymer membrane. The described conditions mimic the physiological conditions that transpire throughout the gastrointestinal tract. The processes that occur in the unstirred aqueous layer are simulated with the use of a plasma-treated membrane in the dissolution apparatus. The biomimetic membrane creates an environment in which free/dissolved drug and drug-containing species enter the membrane through a porous hydrophilic surface and traverse to a hydrophobic surface based on the high partition coefficient of the drug in the selected system. The apparatus and model present the ability to understand the kinetics and mechanisms of dissolution, supersaturation, and nucleation. The utility of the presented method is seen during the evaluation of ASDs of felodipine produced by spray drying and hot melt extrusion. The membrane permeation dissolution apparatus can suggest formulation performance and be employed as a screening tool for selection of candidates to move forward to pharmacokinetic studies. The present model warrants high-throughput analysis and is a cost-effective technique. Future studies will focus on IVIVC of similar formulations to further confirm the versatility and accuracy of the proposed membrane permeation dissolution apparatus for evaluation of *in vivo* performance and free drug dissolution.

## ACKNOWLEDGEMENTS

The authors wish to gratefully acknowledge the financial support of Hovione LLC. The authors would also like to thank Dr. Bruce Weber for his critical review of this manuscript.

## REFERENCES

1. Dahan A, Hoffman A. The effect of different lipid based formulations on the oral absorption of lipophilic drugs: the ability of *in vitro* lipolysis and consecutive *ex vivo* intestinal permeability data to predict *in vivo* bioavailability in rats. *Eur J Pharm Biopharm.* 2007;67(1):96–105.
2. Dahan A, Miller JM. The solubility–permeability interplay and its implications in formulation design and development for poorly soluble drugs. *AAPS J.* 2012;14(2):244–51.
3. Gao Y, Carr RA, Spence JK, Wang WW, Turner TM, Lipari JM, et al. A pH-dilution method for estimation of biorelevant drug solubility along the gastrointestinal tract: application to physiologically based pharmacokinetic modeling. *Mol Pharm.* 2010;7(5):1516–26.
4. Lipinski CA, Lombardo F, Dominy BW, Feeney PJ. Experimental and computational approaches to estimate solubility and permeability in drug discovery and development settings. *Adv Drug Deliv Rev.* 2012;64:4–17.
5. Hughey JR. Chapter 12: dissolution of stabilized amorphous drug formulations. *Poorly soluble drugs: dissolution and drug release:* Pan Stanford Publishing; 2017. p. 393–418.
6. O'Donnell KP, Williams III RO. Optimizing the formulation of poorly water-soluble drugs. *Formulating poorly water soluble drugs:* Springer; 2012. p. 27–93.
7. Thayer AM. Finding solutions. *Chemical & Engineering News.* 2010;88(22):13–8.
8. Dressman JB, Amidon GL, Reppas C, Shah VP. Dissolution testing as a prognostic tool for oral drug absorption: immediate release dosage forms. *Pharm Res.* 1998;15(1):11–22.
9. Azarmi S, Roa W, Löbenberg R. Current perspectives in dissolution testing of conventional and novel dosage forms. *Int J Pharm.* 2007;328(1):12–21.
10. Amidon GL, Sinko PJ, Fleisher D. Estimating human oral fraction dose absorbed: a correlation using rat intestinal membrane permeability for passive and carrier-mediated compounds. *Pharm Res.* 1988;5(10):651–4.
11. Tsume Y, Mudie DM, Langguth P, Amidon GE, Amidon GL. The Biopharmaceutics Classification System: subclasses for *in vivo* predictive dissolution (IPD) methodology and IVIVC. *Eur J Pharm Sci.* 2014;57:152–63.
12. Gautschi JT. Nonsink *in vitro* dissolution testing of amorphous solid dispersions. *Melt extrusion:* Springer; 2013. p. 205–20.
13. Friesen DT, Shanker R, Crew M, Smithey DT, Curatolo W, Nightingale J. Hydroxypropyl methylcellulose acetate succinate-based spray-dried dispersions: an overview. *Mol Pharm.* 2008;5(6):1003–19.
14. Wu B, Li J, Wang Y. Evaluation of the microcentrifuge dissolution method as a tool for spray-dried dispersion. *AAPS J.* 2016;18(2):346–53.
15. Kuentz M. Analytical technologies for real-time drug dissolution and precipitation testing on a small scale. *J Pharm Pharmacol.* 2015;67(2):143–59.
16. Curatolo W, Nightingale JA, Herbig SM. Utility of hydroxypropylmethylcellulose acetate succinate (HPMCAS) for initiation and maintenance of drug supersaturation in the GI milieu. *Pharm Res.* 2009;26(6):1419–31.
17. Wallace SJ, Li J, Nation RL, Boyd BJ. Drug release from nanomedicines: selection of appropriate encapsulation and release methodology. *Drug Deliv Transl Res.* 2012;2(4):284–92.
18. McAllister M. Dynamic dissolution: a step closer to predictive dissolution testing? *Mol Pharm.* 2010;7(5):1374–87.

19. Fyfe C, Grondey H, Blazek-Welsh A, Chopra S, Fahie B. NMR imaging investigations of drug delivery devices using a flow-through USP dissolution apparatus. *J Control Release*. 2000;68(1):73–83.
20. Hong J, Shah JC, Mcgonagle MD. Effect of cyclodextrin derivation and amorphous state of complex on accelerated degradation of ziprasidone. *J Pharm Sci*. 2011;100(7):2703–16.
21. Phillips DJ, Pygall SR, Cooper VB, Mann JC. Overcoming sink limitations in dissolution testing: a review of traditional methods and the potential utility of biphasic systems. *J Pharm Pharmacol*. 2012;64(11):1549–59.
22. Shi Y, Gao P, Gong Y, Ping H. Application of a biphasic test for characterization of in vitro drug release of immediate release formulations of celecoxib and its relevance to in vivo absorption. *Mol Pharm*. 2010;7(5):1458–65.
23. Phillips DJ, Pygall SR, Cooper VB, Mann JC. Toward biorelevant dissolution: application of a biphasic dissolution model as a discriminating tool for HPMC matrices containing a model BCS class II drug. *Dissolution Technol*. 2012;19(1):25–34.
24. Alonzo DE, Gao Y, Zhou D, Mo H, Zhang GG, Taylor LS. Dissolution and precipitation behavior of amorphous solid dispersions. *J Pharm Sci*. 2011;100(8):3316–31.
25. Artursson P, Palm K, Luthman K. Caco-2 monolayers in experimental and theoretical predictions of drug transport. *Adv Drug Deliv Rev*. 2001;46(1):27–43.
26. Kansy M, Senner F, Gubernator K. Physicochemical high throughput screening: parallel artificial membrane permeation assay in the description of passive absorption processes. *J Med Chem*. 1998;41(7):1007–10.
27. Macheras P, Karalis V, Valsami G. Keeping a critical eye on the science and the regulation of oral drug absorption: a review. *J Pharm Sci*. 2013;102(9):3018–36.
28. Obeso CG, Sousa MP, Song W, Rodriguez-Pérez MA, Bhushan B, Mano JF. Modification of paper using polyhydroxybutyrate to obtain biomimetic superhydrophobic substrates. *Colloids Surf A Physicochem Eng Asp*. 2013;416:51–5.
29. Scholz A, Abrahamsson B, Diebold SM, Kostewicz E, Polentarutti BI, Ungell A-L, et al. Influence of hydrodynamics and particle size on the absorption of felodipine in labradors. *Pharm Res*. 2002;19(1):42–6.
30. Dailymed. Felodipine Extended Release Tablets. 2007.
31. van De Waterbeemd H, Camenisch G, Folkers G, Raevsky OA. Estimation of Caco-2 cell permeability using calculated molecular descriptors. *Quantitative Structure-Activity Relationships*. 1996;15(6):480–90.
32. Shah N, Sandhu H, Choi DS, Chokshi H, Malick AW. *Amorphous solid dispersions. Theory and practice*: Springer; 2014.
33. Galia E, Nicolaidis E, Hörter D, Löbenberg R, Reppas C, Dressman J. Evaluation of various dissolution media for predicting in vivo performance of class I and II drugs. *Pharm Res*. 1998;15(5):698–705.
34. Fagerberg JH, Tsinman O, Sun N, Tsinman K, Avdeef A, Bergström CA. Dissolution rate and apparent solubility of poorly soluble drugs in biorelevant dissolution media. *Mol Pharm*. 2010;7(5):1419–30.
35. Reppas C, Vertzoni M. Biorelevant in-vitro performance testing of orally administered dosage forms. *J Pharm Pharmacol*. 2012;64(7):919–30.
36. Vertzoni M, Fotaki N, Nicolaidis E, Reppas C, Kostewicz E, Stippler E, et al. Dissolution media simulating the intraluminal composition of the small intestine: physiological issues and practical aspects. *J Pharm Pharmacol*. 2004;56(4):453–62.
37. Lue B-M, Nielsen FS, Magnussen T, Schou HM, Kristensen K, Jacobsen LO, et al. Using biorelevant dissolution to obtain IVIVC of solid dosage forms containing a poorly-soluble model compound. *Eur J Pharm Biopharm*. 2008;69(2):648–57.
38. Tang L, Khan SU, Muhammad NA. Evaluation and selection of bio-relevant dissolution media for a poorly water-soluble new chemical entity. *Pharm Dev Technol*. 2001;6(4):531–40.
39. Ross MH, Pawlina W. *Histology*: Lippincott Williams & Wilkins; 2006.
40. Simons K, Van Meer G. Lipid sorting in epithelial cells. *Biochemistry*. 1988;27(17):6197–202.
41. Karlsson J, Artursson P. A method for the determination of cellular permeability coefficients and aqueous boundary layer thickness in monolayers of intestinal epithelial (Caco-2) cells grown in permeable filter chambers. *Int J Pharm*. 1991;71(1–2):55–64.
42. Won D-H, Kim M-S, Lee S, Park J-S, Hwang S-J. Improved physicochemical characteristics of felodipine solid dispersion particles by supercritical anti-solvent precipitation process. *Int J Pharm*. 2005;301(1):199–208.
43. Mu L, Feng S. Fabrication, characterization and in vitro release of paclitaxel (Taxol®) loaded poly (lactic-co-glycolic acid) microspheres prepared by spray drying technique with lipid/cholesterol emulsifiers. *J Control Release*. 2001;76(3):239–54.
44. Riddick TM. Control of colloid stability through zeta potential. *Blood*. 1968;10(1).
45. Sugano K, Okazaki A, Sugimoto S, Tavornvipas S, Omura A, Mano T. Solubility and dissolution profile assessment in drug discovery. *Drug Metab Pharmacokinet*. 2007;22(4):225–54.
46. Martinez MN, Amidon GL. A mechanistic approach to understanding the factors affecting drug absorption: a review of fundamentals. *J Clin Pharmacol*. 2002;42(6):620–43.
47. Raina SA, Zhang GG, Alonzo DE, Wu J, Zhu D, Catron ND, et al. Enhancements and limits in drug membrane transport using supersaturated solutions of poorly water-soluble drugs. *J Pharm Sci*. 2013.
48. Jackson MJ, Kestur US, Hussain MA, Taylor LS. Dissolution of danazol amorphous solid dispersions: supersaturation and phase behavior as a function of drug loading and polymer type. *Mol Pharm*. 2015;13(1):223–31.
49. Nejdforss P, Ekelund M, Jeppsson B, Weström B. Mucosal in vitro permeability in the intestinal tract of the pig, the rat, and man: species- and region-related differences. *Scand J Gastroenterol*. 2000;35(5):501–7.
50. Bland JM, Altman D. Statistical methods for assessing agreement between two methods of clinical measurement. *Lancet*. 1986;327(8476):307–10.